Computational modelling of thermoforming processes in the case of finite viscoelastic materials

M. Karamanou [a], M.K. Warby [a] and J.R. Whiteman [a]

[a] *BICOM, Mathematical Sciences,*
Brunel University, Uxbridge, England, UB8 3PH
www.brunel.ac.uk/~icsrbicm

Abstract

In this paper we describe the computational simulation of the inflation phase of a thermoforming process under which a thin polymer sheet is deformed into a mould under the action of applied pressure. It is assumed that the sheet undergoes finite viscoelastic deformation which is treated using a hyperelastic model containing internal variables. The simplification is adopted that the sheet can be treated as a membrane and also that there is a total sticking contact condition when the sheet comes in contact with the mould. The computational model uses finite elements in space and incorporates mesh adaptivity based on a residual estimator in order to simulate the deformation accurately and efficiently. The internal variables satisfy an ordinary differential equation in time which is solved using a predictor-corrector scheme. The constitutive model is a generalisation of that of Le Tallec and Rahier (Int. J. Numer. Meth. Eng. 37, 1159-1186, 1994). In the simulation it is demonstrated how effectively the estimator works in controlling the meshes for some demanding mould shapes.

Key words: Thermoforming, membranes, finite strain, viscoelasticity, adaptivity
1991 MSC: 73F15, 45D05, 65M60

⋆ The authors would like to acknowledge the support of the UK's **Engineering and Physical Sciences Research Council** (GR/R10844/01 and GR/M38070).

Email addresses: marianna.karamanou@brunel.ac.uk (M. Karamanou), mike.warby@brunel.ac.uk (M.K. Warby), john.whiteman@brunel.ac.uk (J.R. Whiteman).

1 Introduction

In this paper we consider various aspects of the computational simulation of the inflation phase of a thermoforming process under which a thin polymer sheet is deformed into a mould under the action of applied pressure. The mathematical model of this process requires that account is taken of the large deformation, the material properties of the polymers and the contact between the sheet and the mould. In the computations a strategy for adaptively refining the meshes in a finite element implementation in space is described, in an attempt to ensure that the calculations are undertaken efficiently and accurately. The new aspects of this work are the use of a finite viscoelastic model of differential type for the material, together with a residual based error estimator which is used to control the meshes in the computations, and the application of a finite viscoelastic model to the thermoforming process.

In the literature there are a number of references to computational models of various implementations of thermoforming with many of the early references being to the group of De Lorenzi [12,4,11,10] from the late 1980's and 1990's. In much of this work a membrane model is used for the sheet, hyperelastic constitutive relations are used for the polymers and a condition of total sticking is used to model the manner in which the sheet comes into contact with the mould. Finite elastic models based on these assumptions are fairly successful in many situations with the more recent efforts at modelling thermoforming being in the case of multi-layer sheets, in the use of other constitutive relations and in the use of contact conditions other than that of total sticking, see e.g. [1,13,5]. The decision as to which effects are important for a realistic simulation is usually an open question, as all contribute in some way to the final outcome. However, it should be noted that when the process is implemented at a modest temperature (well below the melt point of the polymer), it is believed that frictional contact effects are important with the materials being deformed showing very little in the way of rate dependence. At high temperatures close to the melt point it is believed that total sticking contact condition is realistic and in uniaxial material tests significant rate effects are observed in the materials. It is this high temperature version which we consider here, using a finite viscoelastic model which is of the same form as that considered previously by Le Tallec in [6] in a different context. As we explain, this finite constitutive model is basically a hyperelastic model containing an internal variable which satisfies an ordinary differential equation (ODE) which governs how it evolves in time. This structure of the constitutive model allows us to perform computations by combining an elastic solver with a predictor corrector procedure for dealing with changes with time of the internal variable. The constitutive model is thus fairly straightforward to use with only a modest increase in computational effort. As it turns out, all the results obtained suggest that the inclusion of the viscoelastic model, instead of just using a

hyperelastic model, appears to have very little effect on the final deformation that occurs as the sheet is forced against the mould. However id does enable the stress field to be more accurately determined. This outcome is as yet not understood.

The computational effort in a simulation depends mainly on the number of unknowns in the finite element model and this in turn depends on the accuracy that is required. In this paper we describe a residual based error estimator for use in this context to determine which sequence of space meshes should be used to attempt to get a "realistic simulation" in an efficient way in terms of the number of unknowns. We derive the estimator which is applicable to nonlinear elastic models by appropriately linearising at each stage (i.e. at each time level) and then applying error analysis techniques commonly used for linear problems. As we explain, the assumptions used to derive the estimator will often not be met in practice but nevertheless in the results presented the estimator appears to perform well in that it picks out the part of the sheet that stretches the most and which makes contact with the more difficult geometrical features of the mould shapes.

The presentation is as follows. In section 2 we describe the finite membrane deformation together with the viscoelastic constitutive model that we use. In section 3 we outline how we couple the finite element method in space with a predictor corrector type ODE solver in time for the constrained inflation problem. Section 4 then contains details of the residual based estimator and finally in section 5 we show how this performs in the case of a few moderately demanding mould shapes.

2 Finite deformations and a finite viscoelastic constitutive model

In this section we describe the finite viscoelastic membrane model that we use to approximately simulate the deformation during the thermoforming inflation process.

2.1 The deformation, stretching and stress quantities used

As is common with solids we use a Lagrangian description of the large deformation which, for the spatial description of quantities, involves referring everything to the reference state. If $\underline{x}$ denotes the reference position of a typical point in a body then during the deformation we have

$$\underline{x} \to \underline{x} + \underline{u} =: \underline{w}, \quad \underline{x} = (x_i), \quad \underline{u} = (u_i), \quad \underline{w} = (w_i) \tag{1}$$

where $\underline{u} = \underline{u}(\underline{x}, t)$ denotes the displacement at time t. The spatial partial derivatives of this give the deformation gradient $\mathbf{F} = (\partial w_i/\partial x_j)$ and from this we get the right and left Cauchy Green deformation tensors $\mathbf{C} = \mathbf{F}^T\mathbf{F}$ and $\mathbf{B} = \mathbf{F}\,\mathbf{F}^T$. The tensor $\mathbf{F}$ has the polar decomposition $\mathbf{F} = \mathbf{R}\,\mathbf{U} = \mathbf{V}\,\mathbf{R}$ where $\mathbf{R}$ is a proper orthogonal tensor and $\mathbf{U}$ and $\mathbf{V}$ are both symmetric positive definite tensors. For later reference when we refer to isotropic materials we also let here λ_1, λ_2 and λ_3 denote the eigenvalues of $\mathbf{U}$ (which are the same as the eigenvalues of $\mathbf{V}$) which are also known as the principal stretches in this context. The tensors $\mathbf{F}$, $\mathbf{C}$, $\mathbf{B}$, $\mathbf{R}$, $\mathbf{U}$ and $\mathbf{V}$ and the scalars λ_1, λ_2 and λ_3 are all used to describe the stretching that occurs. As we are dealing with viscoelastic materials we also need to take account of the rate at which the sheet is deforming and the usual quantities to describe this are the rate of deformation tensor

$$\mathbf{L} = \left(\frac{\partial \dot{w}_i}{\partial w_j}\right) = \dot{\mathbf{F}}\,\mathbf{F}^{-1} \tag{2}$$

together with

$$\mathbf{D} = \frac{1}{2}\left(\mathbf{L} + \mathbf{L}^T\right) = \frac{1}{2}\left(\dot{\mathbf{F}}\,\mathbf{F}^{-1} + \mathbf{F}^{-T}\dot{\mathbf{F}}\right). \tag{3}$$

For later reference observe that $\dot{\mathbf{C}}$ and $\mathbf{D}$ are related by

$$\dot{\mathbf{C}} = \dot{\mathbf{F}}^T\mathbf{F} + \mathbf{F}^T\dot{\mathbf{F}} = 2\mathbf{F}^T\mathbf{D}\,\mathbf{F}. \tag{4}$$

The stress obtained depends on the constitutive model, which we describe in subsection 2.3, and is given by using the symmetric Cauchy stress $\boldsymbol{\sigma}$ or equivalently by using the non-symmetric nominal stress $\boldsymbol{\Pi} = (\det \mathbf{F})\mathbf{F}^{-1}\boldsymbol{\sigma}$, the first Piola stress $\boldsymbol{\Pi}^T$ or the second Piola stress $\mathbf{S} = (\det \mathbf{F})\mathbf{F}^{-1}\boldsymbol{\sigma}\mathbf{F}^{-T}$. When we have a general three-dimensional body and no body forces, the stresses obtained must satisfy the equations of motion

$$\rho \dot{w}_i = \sum_{j=1}^{3} \frac{\partial \sigma_{ij}}{\partial w_j}, \quad i = 1, 2, 3, \tag{5}$$

where ρ denotes the density, which reduces to the equilibrium equations for quasi-static problems which we consider here. In terms of spatial derivatives with respect to x_1, x_2 and x_3 (i.e. the undeformed coordinates) the equations of quasi-static equilibrium are

$$\sum_{j=1}^{3} \frac{\partial \Pi_{ij}}{\partial x_j} = 0, \quad i = 1, 2, 3. \tag{6}$$

2.2 The membrane simplification

All the details given above are the standard quantities used to describe general finite deformations. In the context of the thermoforming of thin sheets at high temperatures the sheets can sustain little or no bending moments and as a consequence we use the simplifying assumption that the sheet deforms like a membrane. This simplifying assumption allows us to model the three dimensional deformation in a two dimensional way as we now describe.

We assume that the undeformed sheet, which is our reference state, has uniform thickness h_0 and occupies the region

$$\mathcal{B} = \{(x_1, x_2, x_3) : \quad \underline{x} = (x_1, x_2)^T \in \Omega,\ |x_3| < h_0/2\} \tag{7}$$

which has mid-surface $x_3 = 0$. This mid-surface deforms according to

$$(x_1, x_2, 0) \to (x_1 + u_1, x_2 + u_2, u_3) \tag{8}$$

and since material fibres normal to the mid-surface are assumed to remain normal to the sheet throughout the deformation we get a two dimensional description with $\underline{u} = \underline{u}(\underline{x})$. The assumption that the membrane cannot support bending implies that $\boldsymbol{\sigma}\underline{n} = \underline{0}$ where $\underline{n}$ is the unit normal to the mid-surface. With the membrane simplification $\mathbf{C}$ and $\boldsymbol{\sigma}$ hence have the form

$$\mathbf{C} = \mathbf{F}^T\mathbf{F} = \begin{pmatrix} c_{11} & c_{12} & 0 \\ c_{12} & c_{22} & 0 \\ 0 & 0 & \lambda_3^2 \end{pmatrix} \quad \text{and} \quad \mathbf{R}^T\boldsymbol{\sigma}\mathbf{R} = \begin{pmatrix} \tilde{\sigma}_{11} & \tilde{\sigma}_{12} & 0 \\ \tilde{\sigma}_{12} & \tilde{\sigma}_{22} & 0 \\ 0 & 0 & 0 \end{pmatrix} \tag{9}$$

and with the incompressibility assumption $\det \mathbf{C} = \lambda_3^2(c_{11}c_{22} - c_{12}^2) = 1$. Hence with the incompressible membrane there are just 3 stretching components c_{11}, c_{12} and c_{22}, and 3 stress components $\tilde{\sigma}_{11}$, $\tilde{\sigma}_{12}$ and $\tilde{\sigma}_{22}$ to consider.

To obtain the weak form of the equations of equilibrium in this context in the case of an applied pressure of magnitude P as the loading we take the scalar product of (6) with a test vector $\underline{v}$ and integrate over the domain Ω and through the thickness $|x_3| < h_0/2$. This gives

$$a(\underline{u}, \underline{v}) - Pb(\underline{u}, \underline{v}) = 0, \quad \forall \underline{v} \in V \tag{10}$$

where

$$V = H_0^1(\Omega) = \{\underline{v} = (v_i) : \quad v_i \in H^1(\Omega),\ v_i(\underline{x}) = 0,\ \underline{x} \in \partial\Omega\}, \tag{11}$$

where

$$a(\underline{u},\underline{v}) = \iint_\Omega h_0(\mathbf{\Pi}^T : \boldsymbol{\nabla}\underline{v})\, dx_1 dx_2, \tag{12}$$

$$b(\underline{u},\underline{v}) = \iint_\Omega \underline{v} \cdot \left(\frac{\partial \underline{w}}{\partial x_1} \times \frac{\partial \underline{w}}{\partial x_2}\right) dx_1 dx_2 \tag{13}$$

and where in this membrane simplification we now have

$$\mathbf{\Pi}^T = \begin{pmatrix} \Pi_{11} & \Pi_{21} \\ \Pi_{12} & \Pi_{22} \\ \Pi_{13} & \Pi_{23} \end{pmatrix} \quad \text{and} \quad \nabla\underline{v} = \begin{pmatrix} \frac{\partial v_1}{\partial x_1} & \frac{\partial v_1}{\partial x_2} \\ \frac{\partial v_2}{\partial x_1} & \frac{\partial v_2}{\partial x_2} \\ \frac{\partial v_3}{\partial x_1} & \frac{\partial v_3}{\partial x_2} \end{pmatrix} \tag{14}$$

with $\mathbf{\Pi}^T : \nabla\underline{v} = \mathrm{tr}(\mathbf{\Pi} : \nabla\underline{v})$. The operation : is an inner product on quantities of this type. For later reference we also note that, by application of the divergence theorem and making use of the boundary conditions, we can also express $b(\underline{u},\underline{v})$ in the form

$$3b(\underline{u},\underline{v}) = \iint_\Omega \left\{ \underline{v} \cdot \left(\frac{\partial \underline{w}}{\partial x_1} \times \frac{\partial \underline{w}}{\partial x_2}\right) + \underline{w} \cdot \left(\frac{\partial \underline{v}}{\partial x_1} \times \frac{\partial \underline{w}}{\partial x_2} + \frac{\partial \underline{w}}{\partial x_1} \times \frac{\partial \underline{v}}{\partial x_2}\right) \right\} dx_1 dx_2. \tag{15}$$

It is also worth noting here that, by using the divergence theorem again, we obtain the partial differential equation associated with (10) as

$$\nabla \cdot \mathbf{\Pi}^T + P\left(\frac{\partial \underline{w}}{\partial x_1} \times \frac{\partial \underline{w}}{\partial x_2}\right) = \underline{0} \quad \text{where} \quad \nabla \cdot \mathbf{\Pi}^T = \begin{pmatrix} \frac{\partial \Pi_{11}}{\partial x_1} + \frac{\partial \Pi_{21}}{\partial x_2} \\ \frac{\partial \Pi_{12}}{\partial x_1} + \frac{\partial \Pi_{22}}{\partial x_2} \\ \frac{\partial \Pi_{13}}{\partial x_1} + \frac{\partial \Pi_{23}}{\partial x_2} \end{pmatrix}. \tag{16}$$

We need this when we describe our error estimator.

2.3 The finite viscoelastic constitutive model

To complete the description of the unconstrained inflation of a membrane we need constitutive equations which relate the stress at the current time t to the stretching of the material involved. For elastic materials the relations are only between the current stress and the current stretching but for viscoelastic materials the current stress also depends on the entire history of the deformation. We consider here briefly what this involves in general and then outline the finite viscoelastic model that we have been using which is based on a finite deformation generalization of a spring and dashpot model as has previously

been used by Le Tallec in [6] in the context of modelling rubber types. In fact we generalise slightly that given in [6] by considering the case of any type of elastic springs.

2.3.1 Some general principles

In continuum mechanics the starting point for a theoretical derivation of constitutive models is through energy statements such as the first and second laws of thermodynamics. The first law gives a balance of all the energies involved whilst the second law leads to an inequality which is concerned with certain processes only being possible in certain directions. To show what these mean in the context of constitutive models consider an arbitrary volume V of material and suppose that the set-up is such that the only energy transfers to the material in V are due to the mechanical work done by the surface tractions on the boundary of V, the body forces in V and by the heat transfer through the boundary of V. As is shown in standard texts, see e.g. Malvern [8, p.227–], the power input into V, due to mechanical effects, can be written as

$$P_{\text{input}} = \frac{\mathrm{d}}{\mathrm{d}t}\left\{\int_V \frac{1}{2}\rho|\underline{\dot{w}}|^2\,\mathrm{d}V\right\} + \int_V \boldsymbol{\sigma} : \mathbf{D}\,\mathrm{d}V \tag{17}$$

and if $\underline{q}$ denotes the heat flux then the heat input rate can be written as

$$Q_{\text{input}} = -\int_V \nabla \cdot \underline{q}\,\mathrm{d}V. \tag{18}$$

The total power input is $P_{\text{input}} + Q_{\text{input}}$ and the first law of thermodynamics is about the existence of a total energy function E_{total} such that

$$\dot{E}_{\text{total}} = P_{\text{input}} + Q_{\text{input}}. \tag{19}$$

As the first part of (17) (the kinetic energy term) already contains a time derivative this in turn leads to the existence of an internal energy e such that

$$\frac{\mathrm{d}}{\mathrm{d}t}\left\{\int_V \rho e\,\mathrm{d}V\right\} = \int_V \left(\boldsymbol{\sigma} : \mathbf{D} - \nabla \cdot \underline{q}\right)\,\mathrm{d}V \tag{20}$$

from which we get the field equation

$$\rho\frac{\mathrm{d}e}{\mathrm{d}t} = \boldsymbol{\sigma} : \mathbf{D} - \nabla \cdot \underline{q}. \tag{21}$$

In the case of a hyperelastic material and in the case $\underline{q} = \underline{0}$ and with ρ_0 denoting the undeformed density of the material the quantity $W = \rho_0 e$ is known as the strain energy function and we have the usual relation

$$\frac{\rho}{\rho_0}\frac{\mathrm{d}W}{\mathrm{d}t} = \boldsymbol{\sigma} : \mathbf{D} \tag{22}$$

which is the starting point used to derive the stress stretch relations for hyperelastic materials. Here, $W = W(\mathbf{C})$, i.e. the strain energy only depends on the current stretching in the body. Note that since $\det \mathbf{F} = \rho_0/\rho$ it follows from the connection between $\boldsymbol{\sigma}$ and $\mathbf{S}$ that

$$\frac{\rho}{\rho_0}\boldsymbol{\sigma} : \mathbf{D} = \mathrm{tr}\left((\mathbf{F}\,\mathbf{S}\mathbf{F}^T)\left(\frac{1}{2}\mathbf{F}^{-T}\dot{\mathbf{C}}\,\mathbf{F}^{-1}\right)\right) = \frac{1}{2}\mathrm{tr}(\mathbf{S}\,\dot{\mathbf{C}}) = \frac{1}{2}\mathbf{S} : \dot{\mathbf{C}}. \tag{23}$$

Then by using the chain rule to re-express (22) gives

$$\left(\frac{\rho}{\rho_0}\frac{\partial W}{\partial \mathbf{C}} - \mathbf{S}\right) : \dot{\mathbf{C}} = 0. \tag{24}$$

When we have an incompressible material we have that $\det \mathbf{F} = 1$ and in terms of rates we equivalently have $\mathrm{tr}\mathbf{D} = 0$. Now as $2\mathbf{D} = \mathbf{F}^{-T}\dot{\mathbf{C}}\,\mathbf{F}^{-1}$ is similar to $\dot{\mathbf{C}}\,\mathbf{C}^{-1}$, and hence has the same trace, we can write this as

$$\mathrm{tr}(\dot{\mathbf{C}}\mathbf{C}^{-1}) = \mathbf{C}^{-1} : \dot{\mathbf{C}} = 0. \tag{25}$$

Thus the requirement that (24) is true for all possible incompressible deformations implies that $\mathbf{S}$ is of the form

$$\mathbf{S} = -p\mathbf{C}^{-1} + \frac{\partial W}{\partial \mathbf{C}} \tag{26}$$

where p is a hydrostatic pressure term which is not determined by the local deformation in general. In the particular case of a membrane deformation p is however determined so that the stress is consistent with the requirement that $\boldsymbol{\sigma}\underline{n} = \underline{0}$.

In the case of a viscoelastic material we also need to take account of the second law of thermodynamics to see what constraints this imposes on any proposed model. This law is usually expressed mathematically using entropy. With e denoting the internal energy density we let

$$\psi = e - s\theta \tag{27}$$

denote the Helmholtz free energy where s is entropy and θ is temperature. This is the part of the internal energy capable of bring converted into mechanical work. The energy balance relation (21) now becomes

$$\rho\frac{\mathrm{d}\psi}{\mathrm{d}t} + s\dot{\theta} + \dot{s}\theta = \frac{1}{2}\mathbf{S} : \dot{\mathbf{C}} - \nabla \cdot \underline{q}. \tag{28}$$

The second law of thermodynamics implies that every possible deformation and change of state of the material must be such that $\dot{s} \geq 0$, i.e. the entropy s remains constant or increases. Thus if ψ is of the form $\psi = \psi(\mathbf{C}, \mathbf{A}, \theta)$, where

$\mathbf{A}$ denotes any internal variable, then we have

$$\left(\rho\frac{\partial\psi}{\partial\mathbf{C}}-\frac{1}{2}\mathbf{S}\right):\dot{\mathbf{C}}+\left(\rho\frac{\partial\psi}{\partial\theta}+s\right)\dot{\theta}+\rho\frac{\partial\psi}{\partial\mathbf{A}}:\dot{\mathbf{A}}+\nabla\cdot\underline{q}=-\theta\dot{s}\leq 0. \tag{29}$$

For this to hold for all possible changes of state, which includes that in which $\dot{\theta}=0$ and $\underline{q}=\underline{0}$, we must have

$$\mathbf{S}=-p\mathbf{C}^{-1}+2\rho\frac{\partial\psi}{\partial\mathbf{C}}\quad\text{and}\quad-\frac{\partial\psi}{\partial\mathbf{A}}:\dot{\mathbf{A}}\geq 0, \tag{30}$$

where, as in the elastic case, p is a hydrostatic pressure term.

Thus, to summarise, in the case of deformations at constant temperature θ involving no heat flow the hyperelastic case occurs when $\psi=\psi(\mathbf{C})$ and we get (26) whereas for a viscoelastic material we have instead $\psi=\psi(\mathbf{C},\mathbf{A})$ leading to (30). The term

$$-\rho\frac{\partial\psi}{\partial\mathbf{A}}:\dot{\mathbf{A}}\geq 0 \tag{31}$$

is known as the dissipation and the inequality indicates the direction that things must happen.

2.3.2 The spring–dashpot model

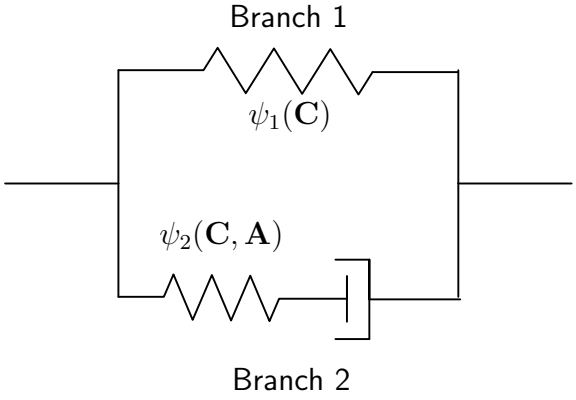

Fig. 1. A spring in parallel with a spring and a dashpot

We now consider a form of ψ consistent with (30) based on a configuration of springs and dashpots similar to that used previously in [6]. Viscoelastic models based on springs and dashpots have been used for some time in the case of small strain and linear problems and these are described in many text books, see e.g. Christensen [3]. With a few adjustments to the details such models can also be generalised to finite deformations with the key adjustment being that an additive decomposition of the small strain used in the linear case is replaced by a multiplicative decomposition of the deformation gradient. The details are as follows.

We restrict to the case of the set-up shown in figure 1 involving an elastic spring in branch 1 in parallel with branch 2 which contains a spring and a dashpot in series. Assuming an incompressible deformation we do a multiplicative decomposition of the deformation gradient $\mathbf{F}$ as

$$\mathbf{F} = \mathbf{F}_e\mathbf{F}_v, \tag{32}$$

with $\mathbf{F}_e$ associated with the spring in branch 2 and with $\mathbf{F}_v$ associated with the dashpot in branch 2 and we additionally assume $\det\mathbf{F}_e = \det\mathbf{F}_v = 1$, i.e. the deformation in each part is incompressible. For later reference each of $\mathbf{F}_e$, $\mathbf{F}_v$ and $\mathbf{F}$ have polar decompositions

$$\mathbf{F}_e = \mathbf{R}_e\mathbf{U}_e, \quad \mathbf{F}_v = \mathbf{R}_v\mathbf{U}_v \quad \text{and} \quad \mathbf{F} = \mathbf{R}\,\mathbf{U} \tag{33}$$

where $\mathbf{R}_e$, $\mathbf{R}_v$ and $\mathbf{R}$ are proper orthogonal tensors and where $\mathbf{U}_e$, $\mathbf{U}_v$ and $\mathbf{U}$ are symmetric and positive definite. With this set-up we define an internal variable by

$$\mathbf{A} = \mathbf{F}_v^T\mathbf{F}_v \tag{34}$$

and with $\mathbf{F}_e(0) = \mathbf{F}(0)$, $\mathbf{F}_v(0) = \mathbf{I}$ we have the initial condition $\mathbf{A}(0) = \mathbf{I}$. Now, associated with $\mathbf{F}_e$ we have $\mathbf{B}_e = \mathbf{F}_e\mathbf{F}_e^T$ and observe that

$$\mathbf{B}_e = \mathbf{F}_e\mathbf{F}_e^T = \mathbf{F}\,\mathbf{F}_v^{-1}\mathbf{F}_v^{-T}\mathbf{F}^T = \mathbf{F}\,\mathbf{A}^{-1}\mathbf{F}^T. \tag{35}$$

If we take the spring in branch 2 to be of the general Ogden form for an incompressible isotropic membrane deformation then we have a strain energy function $\tilde{W}_2 = \rho\psi_2$ of the form $\tilde{W}_2(\tilde{\lambda}_1, \tilde{\lambda}_2)$ where

$$\tilde{W}_2 = \sum_1^N \frac{\mu_p}{\nu_p}\left(\tilde{\lambda}_1^{\nu_p} + \tilde{\lambda}_2^{\nu_p} + \tilde{\lambda}_1^{-\nu_p}\tilde{\lambda}_2^{-\nu_p} - 3\right), \quad \frac{\mu_p}{\nu_p} > 0, \tag{36}$$

where μ_p and ν_p are constants and where $\tilde{\lambda}_1^2$ and $\tilde{\lambda}_2^2$ are the eigenvalues of $\mathbf{B}_e$. If $\underline{\tilde{b}}_1$ and $\underline{\tilde{b}}_2$ are the normalised eigenvectors of $\mathbf{B}_e$ corresponding to $\tilde{\lambda}_1^2$ and $\tilde{\lambda}_2^2$ respectively then the membrane Cauchy stress due to the spring is given by

$$\tilde{\lambda}_1\frac{\partial\tilde{W}_2}{\partial\tilde{\lambda}_1}\underline{\tilde{b}}_1\underline{\tilde{b}}_1^T + \tilde{\lambda}_2\frac{\partial\tilde{W}_2}{\partial\tilde{\lambda}_2}\underline{\tilde{b}}_2\underline{\tilde{b}}_2^T \tag{37}$$

which, by using the spectral decomposition of $\mathbf{B}_e$, can also be expressed in the form

$$-p_e\mathbf{I} + \chi_1\mathbf{B}_e + \chi_{-1}\mathbf{B}_e^{-1}, \quad \text{where } p_e = (\chi_1\mathbf{C}_e + \chi_{-1}\mathbf{C}_e^{-1})_{33}, \tag{38}$$

where here $\mathbf{C}_e = \mathbf{R}^T\mathbf{B}_e\mathbf{R}$ in order to satisfy the membrane stress condition that $\boldsymbol{\sigma}\underline{n} = \underline{0}$. The form (37) (or equivalently (38)) defines a frame invariant stress quantity. The stored energy of this system is ψ where

$$\psi = \psi_1 + \psi_2 \tag{39}$$

with the dissipation of the system being entirely due to the linear viscous dashpot.

To describe the dissipation term we need to consider rate of deformation. Corresponding to what is given in (2)–(4), we have associated with $\mathbf{F}_v$ the terms

$$\mathbf{L}_v = \dot{\mathbf{F}}_v \mathbf{F}_v^{-1} \quad \text{and} \quad \mathbf{D}_v = \frac{1}{2}\left(\mathbf{L}_v + \mathbf{L}_v^T\right) = \frac{1}{2}\mathbf{F}_v^{-T}\dot{\mathbf{A}}\,\mathbf{F}_v^{-1}. \tag{40}$$

A frame invariant Cauchy stress in the case of a linear viscous dashpot with viscosity ν is of the form

$$-p_v\mathbf{I} + 2\nu\mathbf{R}_e\mathbf{D}_v\mathbf{R}_e^T \tag{41}$$

and the associated dissipation is given by

$$2\nu\mathbf{D}_v : \mathbf{D}_v = 2\nu\mathrm{tr}(\mathbf{D}_v^2). \tag{42}$$

The ordinary differential equation (ODE) which governs how $\mathbf{A}$ evolves in time is obtained by balancing the deviatoric parts of the stress terms given in (38) and (41), i.e.

$$(-p_e\mathbf{I} + \chi_1\mathbf{B}_e + \chi_{-1}\mathbf{B}_e^{-1})_D = 2\nu(-p_v\mathbf{I} + \mathbf{R}_e\mathbf{D}_v\mathbf{R}_e^T)_D \tag{43}$$

or alternatively by using the dissipation relation

$$-\rho\frac{\partial\psi}{\partial\mathbf{A}} : \dot{\mathbf{A}} = -\rho\frac{\partial\psi_2}{\partial\mathbf{A}} : \dot{\mathbf{A}} = 2\nu\mathrm{tr}(\mathbf{D}_v^2) \tag{44}$$

which requires that $\nu \geq 0$. We consider here both approaches to deriving an ODE for $\mathbf{A}$.

By using the stress balancing approach and noting that

$$\mathrm{tr}(\mathbf{R}_e\mathbf{D}_v\mathbf{R}_e^T) = \mathrm{tr}(\mathbf{D}_v) = 0 \tag{45}$$

and $2\mathbf{D}_v = \mathbf{F}_v^{-T}\dot{\mathbf{A}}\mathbf{F}_v^{-1}$ the relation (43) becomes

$$\chi_1\mathbf{B}_e + \chi_{-1}\mathbf{B}_e^{-1} - \frac{1}{3}\mathrm{tr}\left(\chi_1\mathbf{B}_e + \chi_{-1}\mathbf{B}_e^{-1}\right)\mathbf{I} = \nu\mathbf{R}_e\mathbf{F}_v^{-T}\dot{\mathbf{A}}\mathbf{F}_v^{-1}\mathbf{R}_e^T \tag{46}$$

which rearranges to

$$\mathbf{F}_v^T\mathbf{R}_e^T(\chi_1\mathbf{B}_e + \chi_{-1}\mathbf{B}_e^{-1})\mathbf{R}_e\mathbf{F}_v - \frac{1}{3}\mathrm{tr}(\chi_1\mathbf{B}_e + \chi_{-1}\mathbf{B}_e^{-1})\mathbf{A} = \nu\dot{\mathbf{A}}. \tag{47}$$

To simplify this further note that

$$\mathbf{F}_v^T\mathbf{R}_e^T\mathbf{B}_e\mathbf{R}_e\mathbf{F}_v = \mathbf{F}_v^T\mathbf{C}_e\mathbf{F}_v = \mathbf{F}_v^T\mathbf{F}_e^T\mathbf{F}_e\mathbf{F}_v = \mathbf{F}^T\mathbf{F} = \mathbf{C}, \tag{48}$$

$$\mathbf{F}_v^T\mathbf{R}_e^T\mathbf{B}_e^{-1}\mathbf{R}_e\mathbf{F}_v = \mathbf{F}_v^T\mathbf{C}_e^{-1}\mathbf{F}_v = \mathbf{F}_v^T\mathbf{F}_v\mathbf{F}_v^{-T}\mathbf{C}_e^{-1}\mathbf{F}_v^{-T}\mathbf{F}_v^T\mathbf{F}_v = \mathbf{A}\mathbf{C}^{-1}\mathbf{A} \tag{49}$$

and $\mathbf{B}_e = \mathbf{F}\,\mathbf{A}^{-1}\mathbf{F}^T$ is similar to $\mathbf{A}^{-1}\mathbf{C}$ and $\mathbf{B}_e^{-1}$ is similar to $\mathbf{C}^{-1}\mathbf{A}$. Thus the ODE for $\mathbf{A}$ in the case of a general spring in branch 2 can be written in the form

$$\nu\dot{\mathbf{A}} = \chi_1\mathbf{C} + \chi_{-1}\mathbf{A}\mathbf{C}^{-1}\mathbf{A} - \frac{1}{3}\mathrm{tr}\left(\chi_1\mathbf{A}^{-1}\mathbf{C} + \chi_{-1}\mathbf{A}\mathbf{C}^{-1}\right)\mathbf{A}, \quad \mathbf{A}(0) = \mathbf{I}. \tag{50}$$

It should be noted here that the scalar terms χ_1 and χ_{-1} also depend on $\mathbf{A}$ as they depend on $\tilde{\lambda}_1$ and $\tilde{\lambda}_2$ from the equivalence of (37) and (38). It is straightforward to evaluate χ_1 and χ_{-1} when needed during computations.

It is also instructive to see how (50) is obtained using (44) and to do this we must first note that

$$\mathbf{B}_e\tilde{\underline{b}}_i = \tilde{\lambda}_i^2\tilde{\underline{b}}_i, \quad \tilde{\underline{b}}_i^T\tilde{\underline{b}}_i = 1 \quad \text{gives } \tilde{\lambda}_i^2 = \tilde{\underline{b}}_i^T\mathbf{B}_e\tilde{\underline{b}}_i = \tilde{\underline{b}}_i^T\mathbf{F}\mathbf{A}^{-1}\mathbf{F}^T\tilde{\underline{b}}_i. \tag{51}$$

Differentiating partially with respect to the coefficients of $\mathbf{A}$ leads to

$$2\tilde{\lambda}_i\frac{\partial\tilde{\lambda}_i}{\partial\mathbf{A}} = -\mathbf{A}^{-1}\mathbf{F}^T\tilde{\underline{b}}_i\tilde{\underline{b}}_i^T\mathbf{F}\,\mathbf{A}^{-1}, \quad i = 1, 2 \tag{52}$$

and then using the chain rule together with $\mathbf{A}^{-1}\mathbf{F}^T\tilde{\underline{b}}_i = \tilde{\lambda}_i^2\mathbf{F}^{-1}\tilde{\underline{b}}_i$ we have with $W_2 = W_2(\mathbf{C}, \mathbf{A}) = \rho\psi_2 = \tilde{W}_2(\tilde{\lambda}_2, \tilde{\lambda}_2)$ that

$$2\frac{\partial W_2}{\partial\mathbf{A}} = 2\left(\frac{\partial\tilde{W}_2}{\partial\tilde{\lambda}_1}\frac{\partial\tilde{\lambda}_1}{\partial\mathbf{A}} + \frac{\partial\tilde{W}_2}{\partial\tilde{\lambda}_2}\frac{\partial\tilde{\lambda}_2}{\partial\mathbf{A}}\right) \tag{53}$$

$$= -\mathbf{F}^{-1}\left(\tilde{\lambda}_1\frac{\partial\tilde{W}_2}{\partial\tilde{\lambda}_1}\tilde{\underline{b}}_1\,\tilde{\underline{b}}_1^T + \tilde{\lambda}_2\frac{\partial\tilde{W}_2}{\partial\tilde{\lambda}_2}\tilde{\underline{b}}_2\,\tilde{\underline{b}}_2^T\right)\mathbf{F}\,\mathbf{A}^{-1}. \tag{54}$$

Using (44) and that

$$4\mathrm{tr}(\mathbf{D}_v^2) = \mathrm{tr}(\dot{\mathbf{A}}\,\mathbf{A}^{-1}\dot{\mathbf{A}}\,\mathbf{A}^{-1}) = (\mathbf{A}^{-1}\dot{\mathbf{A}}\,\mathbf{A}^{-1}) : \dot{\mathbf{A}} \tag{55}$$

we get

$$\mathbf{F}^{-1}\left(\tilde{\lambda}_1\frac{\partial\tilde{W}_2}{\partial\tilde{\lambda}_1}\tilde{\underline{b}}_1\,\tilde{\underline{b}}_1^T + \tilde{\lambda}_2\frac{\partial\tilde{W}_2}{\partial\tilde{\lambda}_2}\tilde{\underline{b}}_2\,\tilde{\underline{b}}_2^T\right)\mathbf{F}\,\mathbf{A}^{-1} : \dot{\mathbf{A}} = \nu\mathbf{A}^{-1}\dot{\mathbf{A}}\,\mathbf{A}^{-1} : \dot{\mathbf{A}}. \tag{56}$$

Since $\det\mathbf{A} = 1$ implies that $\dot{\mathbf{A}} : \mathbf{A} = 0$ the relation (56) being true for all possible such $\mathbf{A}$ implies that

$$\mathbf{F}^{-1}\left(\tilde{\lambda}_1\frac{\partial\tilde{W}_2}{\partial\tilde{\lambda}_1}\tilde{\underline{b}}_1\,\tilde{\underline{b}}_1^T + \tilde{\lambda}_2\frac{\partial\tilde{W}_2}{\partial\tilde{\lambda}_2}\tilde{\underline{b}}_2\,\tilde{\underline{b}}_2^T\right)\mathbf{F}\,\mathbf{A}^{-1} - p\mathbf{A}^{-1} = \nu\mathbf{A}^{-1}\dot{\mathbf{A}}\,\mathbf{A}^{-1}, \tag{57}$$

$$\left(\tilde{\lambda}_1\frac{\partial\tilde{W}_2}{\partial\tilde{\lambda}_1}\tilde{\underline{b}}_1\,\tilde{\underline{b}}_1^T + \tilde{\lambda}_2\frac{\partial\tilde{W}_2}{\partial\tilde{\lambda}_2}\tilde{\underline{b}}_2\,\tilde{\underline{b}}_2^T\right) - p\mathbf{I} = \nu\mathbf{F}\,\mathbf{A}^{-1}\dot{\mathbf{A}}\,\mathbf{F}^{-1} \tag{58}$$

where p is an arbitrary scalar. By taking the deviatoric part to eliminate p and by using the equivalence of (37) and (38) gives

$$\nu\dot{\mathbf{A}} = \mathbf{A}\,\mathbf{F}^{-1}\left(\chi_1\mathbf{B}_e + \chi_{-1}\mathbf{B}_e^{-1}\right)\mathbf{F} - \frac{1}{3}\mathrm{tr}\left(\chi_1\mathbf{B}_e + \chi_{-1}\mathbf{B}_e^{-1}\right)\mathbf{A}. \tag{59}$$

This simplifies to the ODE given in (50) by using (49) and (48) together with the relations

$$\mathbf{A}\,\mathbf{F}^{-1}\mathbf{B}_e\mathbf{F} = \mathbf{C} \quad \text{and} \quad \mathbf{A}\,\mathbf{F}^{-1}\mathbf{B}_e^{-1}\mathbf{F} = \mathbf{A}\,\mathbf{F}^{-1}\mathbf{F}^{-T}\mathbf{A}\,\mathbf{F}^{-1}\mathbf{F} = \mathbf{A}\,\mathbf{C}^{-1}\mathbf{A}. \tag{60}$$

In the above we have considered the stress in branch 2 to obtain the ODE governing how $\mathbf{A}$ evolves in time. The stress of the complete spring and dashpot set-up is a combination of the stress in both branch 1 and branch 2 and to describe this let λ_1^2 and λ_2^2 be the eigenvalues of $\mathbf{B} = \mathbf{F}\,\mathbf{F}^T$ (and also of the 2×2 version of $\mathbf{C}$) with associated normalised eigenvectors $\underline{b}_1$ and $\underline{b}_2$ respectively. If $\tilde{W}_1 = \tilde{W}_1(\lambda_1,\lambda_2)$ is the strain energy function of the spring in branch 1 then we have

$$\boldsymbol{\sigma} = \left(\lambda_1\frac{\partial\tilde{W}_1}{\partial\lambda_1}\underline{b}_1\underline{b}_1^T + \lambda_2\frac{\partial\tilde{W}_1}{\partial\lambda_2}\underline{b}_2\underline{b}_2^T\right) + \left(\tilde{\lambda}_1\frac{\partial\tilde{W}_2}{\partial\tilde{\lambda}_1}\tilde{\underline{b}}_1\tilde{\underline{b}}_1^T + \tilde{\lambda}_2\frac{\partial\tilde{W}_2}{\partial\tilde{\lambda}_2}\tilde{\underline{b}}_2\tilde{\underline{b}}_2^T\right) \tag{61}$$

with $\tilde{\lambda}_1$, $\tilde{\lambda}_2$, $\tilde{\underline{b}}_1$ and $\tilde{\underline{b}}_2$ all depending on $\mathbf{A}$ satisfying the ODE (50).

2.3.3 Other ways of representing the stress

To appreciate the 'elastic way' of writing the relations we give here other ways in which the stress–stretch relations can be written. If for our membrane case we let $W_1 = W_1(\mathbf{C}) = \tilde{W}_1(\lambda_1(\mathbf{C}),\lambda_2(\mathbf{C}))$, by which we mean that W_1 just depends on c_{11}, c_{22}, c_{12} and c_{21}, then we have the spectral decomposition

$$2\mathbf{F}\,\frac{\partial W_1}{\partial\mathbf{C}}\mathbf{F}^T = \lambda_1\frac{\partial\tilde{W}_1}{\partial\lambda_1}\underline{b}_1\underline{b}_1^T + \lambda_2\frac{\partial\tilde{W}_1}{\partial\lambda_2}\underline{b}_2\underline{b}_2^T \tag{62}$$

and similarly if we let $W_2 = W_2(\mathbf{C}_e) = \tilde{W}_2(\tilde{\lambda}_1(\mathbf{C}_e),\tilde{\lambda}_2(\mathbf{C}_e))$ where, as above, the dependence on $\mathbf{C}_e = \mathbf{U}\mathbf{A}^{-1}\mathbf{U}$ is only on the 2×2 principal submatrix of $\mathbf{C}_e$, then

$$2\mathbf{F}_e\,\frac{\partial W_2}{\partial\mathbf{C}_e}\mathbf{F}_e^T = \tilde{\lambda}_1\frac{\partial\tilde{W}_2}{\partial\tilde{\lambda}_1}\tilde{\underline{b}}_1\tilde{\underline{b}}_1^T + \tilde{\lambda}_2\frac{\partial\tilde{W}_2}{\partial\tilde{\lambda}_2}\tilde{\underline{b}}_2\tilde{\underline{b}}_2^T. \tag{63}$$

Further, as $\mathbf{C}_e$ is similar to $\mathbf{C}\mathbf{A}^{-1}$ and to $\mathbf{A}^{-1/2}\mathbf{C}\mathbf{A}^{-1/2}$ we have the eigenvalue/eigenvector relations

$$\mathbf{A}^{-1/2}\mathbf{C}\mathbf{A}^{-1/2}\underline{q}_k = \tilde{\lambda}_k^2\underline{q}_k, \quad \tilde{\lambda}_k^2 = \underline{q}_k^T\mathbf{A}^{-1/2}\mathbf{C}\mathbf{A}^{-1/2}\underline{q}_k, \quad \text{with } \underline{q}_k^T\underline{q}_k = 1 \tag{64}$$

leading to

$$2\tilde{\lambda}_k \frac{\partial \tilde{\lambda}_k}{\partial \mathbf{C}} = \mathbf{A}^{-1/2} \underline{q}_k \underline{q}_k^T \mathbf{A}^{-1/2}. \tag{65}$$

Thus if we now consider W_2 to be a function of c_{11}, c_{22}, c_{12} and c_{21} then

$$2\mathbf{F} \frac{\partial W_2}{\partial \mathbf{C}} \mathbf{F}^T = \sum_{k=1}^{2} \frac{1}{\tilde{\lambda}_k} \frac{\partial \tilde{W}_2}{\partial \tilde{\lambda}_k} \mathbf{F} \mathbf{A}^{-1/2} \underline{q}_k \underline{q}_k^T \mathbf{A}^{-1/2} \mathbf{F}^T \tag{66}$$

$$= \sum_{k=1}^{2} \tilde{\lambda}_k \frac{\partial \tilde{W}_2}{\partial \tilde{\lambda}_k} \underline{\tilde{b}}_k \underline{\tilde{b}}_k^T = 2\mathbf{F}_e \frac{\partial W_2}{\partial \mathbf{C}_e} \mathbf{F}_e^T \tag{67}$$

where the last relation follows by using

$$(\mathbf{U}\,\mathbf{A}^{-1}\mathbf{U})(\mathbf{U}\mathbf{A}^{-1/2}\underline{q}_k) = \tilde{\lambda}_k^2 (\mathbf{U}\mathbf{A}^{-1/2}\underline{q}_k) \tag{68}$$

leading to

$$\mathbf{F}\mathbf{A}^{-1/2}\underline{q}_k = \mathbf{R}\,\mathbf{U}\,\mathbf{A}^{-1/2}\underline{q}_k = \pm\tilde{\lambda}_k \underline{\tilde{b}}_k. \tag{69}$$

The point about presenting these different forms is that with

$$W = W_1(\mathbf{C}) + W_2(\mathbf{C}\,\mathbf{A}^{-1}) \tag{70}$$

the membrane stress given in (61) is of the form

$$\boldsymbol{\sigma} = 2\mathbf{F} \frac{\partial W}{\partial \mathbf{C}} \mathbf{F}^T, \tag{71}$$

i.e. the viscoelastic stress field is also an elastic stress field which depends on $\mathbf{A}$ and it corresponds to a continuously varying elastic material as $\mathbf{A}$ varies in time.

2.4 A summary of the continuous problem and further comments

To gather together the different parts, we have a membrane deformation given by (8) which leads to stretching and stress terms satisfying (9) with the quasi-static equilibrium of the body being described by the relations (10)–(15). With the spring and dashpot set-up we have $\boldsymbol{\Pi}^T = \boldsymbol{\sigma}\,\mathbf{F}^{-T}$ with $\boldsymbol{\sigma}$ of the form given in (61) which is convenient when $\tilde{W}_1$ and $\tilde{W}_2$ are given in Ogden form. For the numerical computations described in the next section it is also worth noting that with $\mathbf{F} \in \mathbb{R}^{3\times 2}$ involving the first two columns of the full three dimensional version of $\mathbf{F}$ we have

$$\boldsymbol{\Pi}^T = \frac{\partial \tilde{W}}{\partial \mathbf{F}} \in \mathbb{R}^{3\times 2} \tag{72}$$

where now $\tilde{W} = \tilde{W}(\mathbf{F})$. As has already been stated W varies with $\mathbf{A}$ and hence we must determine the mid-surface displacement $\underline{u} = \underline{u}(\underline{x}, t)$, and the

internal variable $\mathbf{A} = \mathbf{A}(\underline{x}, t)$, for $\underline{x} = (x_1, x_2)^T \in \Omega$ and for $t \geq 0$ satisfying the relations described above.

3 The numerical scheme

3.1 The finite element discretization combined with the predictor-corrector ODE solver

For the numerical scheme we discretise in both space and in time and we must approximate both the displacement $\underline{u} = \underline{u}(\underline{x}, t)$ and the internal variable $\mathbf{A} = \mathbf{A}(\underline{x}, t)$. We do this in a fairly standard way by having time levels $0 = t_0 < t_1 < \cdots < t_j < \cdots$ and seeking at each time level t_j a piecewise linear finite element function $\underline{u}_h(\underline{x}, t_j)$ and a function $\mathbf{A}_h(\underline{x}, t_j)$, which is constant on each element, satisfying a discrete version of the equilibrium equations together with a finite difference discretization of the ODE (50). To keep the numerical scheme as simple as possible we decouple, as much as possible, these two parts by using a predictor corrector type approach for the ODE. In this way we get a sequence of steps in which we are either just estimating $\mathbf{A}_h(\underline{x}, t_j)$ or we are just solving an elastic type problem for $\underline{u}_h(\underline{x}, t_j)$. The details are as follows.

As we have a Lagrangean description the spatial mesh is of the reference configuration $\Omega \subset \mathbb{R}^2$ and this is done here using nodal points $\underline{x}_1, \cdots, \underline{x}_M$ and linear triangles $\Omega_1, \cdots, \Omega_{\text{ne}}$ (both of which are fixed in time) such that

$$\overline{\Omega} = \bigcup_{k=1}^{\text{ne}} \overline{\Omega}_k, \qquad \Omega_i \cap \Omega_j = \emptyset, \quad \text{for } i \neq j. \tag{73}$$

With respect to the mesh we let $N_1, N_2, \cdots, N_M$ denote the usual linear shape functions satisfy the interpolation conditions $N_i(\underline{x}_k) = \delta_{ik}$. Using these functions we have at any given time t_j that the finite element displacement field $\underline{u}_h(\underline{x})$ is the form

$$\underline{u}_h(\underline{x}) = \sum_{i=1}^{M} \sum_{k=1}^{3} (\underline{u}_h)_{ik} N_i(\underline{x}) \underline{e}_k \tag{74}$$

where $\underline{e}_1$, $\underline{e}_2$ and $\underline{e}_3$ are the cartesian base vectors in $\mathbb{R}^3$, and the test space V_h is given by

$$V_h := \text{span}\{N_i(\underline{x})\underline{e}_k : \ i = 1, \cdots, M, \quad k = 1, 2, 3, \quad \underline{x}_i \notin \partial\Omega\} \subset V. \tag{75}$$

Now assuming that we have an estimate of $\mathbf{A}_h$ throughout Ω at time t_j and with $P = P(t_j)$ being the magnitude of the applied pressure the unknown nodal displacement parameters at time t_j are obtained by solving the nonlinear

system arising from the relation

$$a(\underline{u}_h, \underline{v}) - P(t_j)\underline{b}(\underline{u}_h, \underline{v}) = 0, \quad \forall \underline{v} \in V_h \tag{76}$$

which is the discretised version of (10). The nonlinear system is solved using Newton's method for systems with standard modifications such as not necessarily computing the Jacobian matrix at each iteration, the possible use of damping to increase the likelihood of convergence and with replacing t_j by $(t_j + t_{j-1})/2$ if at any time level the iteration does not converge. It should be noted here that as (76) corresponds to solving an elastic problem (which depends on $\mathbf{A}_h$), where the stress quantities are the partial derivatives of a potential (see (72)) and the $b(.,.)$ term can be written in the form given in (15), the nonlinear system associated with (76) has a symmetric and generally positive definite Jacobian matrix. This is one of the benefits of decoupling, as far as possible, the solution of the spatial problem and the solution of the ODE.

Our predictor–corrector approach for estimating $\mathbf{A}_h$ throughout Ω at time t_j together with how it combines with the elastic solver is as follows. Let $\mathbf{A}_h(\underline{x}, t_{j-1})$ denote the internal variable at time t_{j-1}, let $\Delta t_j = t_j - t_{j-1}$ be the time step and let $\nu\dot{\mathbf{A}} = \mathbf{g}(\mathbf{C}, \mathbf{A})$ denote the ODE given in (50).

Predict step: We predict $\mathbf{A}_h(., t_j)$ element by element using the Euler predictor

$$\mathbf{A}_h^{(0)}(\underline{x}, t_j) := \mathbf{A}_h(\underline{x}, t_{j-1}) + \frac{\Delta t_j}{\nu}\mathbf{g}(\mathbf{C}(\underline{x}, t_{j-1}), \mathbf{A}_h(\underline{x}, t_{j-1})), \tag{77}$$

Evaluate step: We solve the elastic problem using $\mathbf{A}_h^{(0)}(., t_j)$ as our estimate for $\mathbf{A}_h(., t_j)$. From the elastic field we get the approximation $\mathbf{C}^{(1)}(\underline{x}, t_j)$ to the Cauchy Green deformation tensor at time t_j.

Corrector step: Using the displacement field just computed we attempt to improve the estimate of $\mathbf{A}_h(., t_j)$ by using the trapezoidal rule corrector which involves solving the following for $\mathbf{A}_h^{(1)}(\underline{x}, t_j)$.

$$\begin{aligned}&\mathbf{A}_h^{(1)}(\underline{x}, t_j) - \mathbf{A}_h(\underline{x}, t_{j-1}) \\ &-\frac{\Delta t_j}{2\nu}\Big(\mathbf{g}(\mathbf{C}(\underline{x}, t_{j-1}), \mathbf{A}_h(\underline{x}, t_{j-1})) + \mathbf{g}(\mathbf{C}^{(1)}(\underline{x}, t_j), \mathbf{A}_h^{(1)}(\underline{x}, t_j))\Big) = \mathbf{0}.\end{aligned} \tag{78}$$

On each element this is a nonlinear system for the 3 components of $\mathbf{A}_h^{(1)}(\underline{x}, t_j)$ that we need to determine.

Evaluate step: The finite element elastic problem is re-solved using the improved prediction for $\mathbf{A}_h(\underline{x}, t_j)$ from the previous corrector step to get the new approximation for $\underline{u}_h(\underline{x}, t_j)$. The nodal values from the previous evaluate step can be used to generate the start vector for Newton's method to solve the nonlinear equations at this stage which usually leads to less computation being required here than in the first evaluate step.

Further corrector and evaluate steps can be performed but the above is usually sufficient.

3.2 A contact algorithm

In the case of a constrained inflation problem in which a sheet sticks to a mould on contact the equations above just describe the part of the sheet at any given stage which is still free and a complete computational simulation also needs to include an algorithm for dealing with the contact. Although a significant amount of the total computation is concerned with this phase of the deformation an algorithm for dealing with this is reasonably straightforward. The algorithm that we use just needs a description of the mould surface of the form $\phi(\underline{y}) = 0$ where ϕ is such that $\phi(\underline{y}) > 0$ when $\underline{y}$ is inside the mould and $\phi(\underline{y}) < 0$ when $\underline{y}$ is outside the mould. The algorithm is as follows. We let $\Omega_{\text{free}}(t_i)$ denote the part of Ω which is not stuck to the mould which is determined using all the nodal points and associated triangles which are not yet in contact with the mould. Using the region $\Omega_{\text{free}}(t_{j-1})$ we solve the quasi-static equilibrium problem using this domain at time t_j and we then consider each deformed nodal point $\underline{w}_k(t_j) = \underline{x}_k + \underline{u}_h(\underline{x}_k, t_j)$ to check that it is inside or on the mould. If any point $\underline{w}_k(t_j)$ is such that $\phi(\underline{w}_k(t_j)) < 0$ then we determine where the line segment joining $\underline{w}_k(t_{j-1})$ to $\underline{w}_k(t_j)$ cuts the mould. We then change $\underline{u}_h(\underline{x}_k, t_j)$ so that $\underline{x}_k + \underline{u}_h(\underline{x}_k, t_j)$ is exactly at this position on the mould. We constrain all such points $\underline{x}_k$ to generate a smaller region $\Omega_{\text{free}}(t_j)$ and we re-solve the equilibrium equations at time t_j using now $\Omega_{\text{free}}(t_j)$ in order to re-establish equilibrium. We perform this procedure at times $t_0 < t_1 < t_2 < \cdots$ involving pressures $P(t_0) \leq P(t_1) \leq P(t_2) \leq \cdots$ until all the deformed nodal points are stuck to the mould.

4 Error estimation and adaptivity in space

The numerical scheme described in the previous section considered a mesh fixed in time for a sequence of time levels corresponding to a sequence of increasing pressures as the membrane is inflated into a mould. How accurate the approximation $\underline{u}_h$ to $\underline{u}$ is at any given stage depends to a large extent on the mesh used and we are likely to improve the approximation when we refine the mesh. Ideally the refinement should be done adaptively based on some estimate of the error in the approximation and to this end we construct a residual type estimator which we use in this context. Our overall procedure involves solving with a mesh fixed in time for all the time levels until all nodal points are in contact with a mould, using the estimator to determine a new mesh and then solving again with this new mesh. This procedure is repeated

until the estimate of the error is sufficiently small.

Residual based estimators have been used for some time for linear problems where the theory is well established and where results can be proved but for nonlinear problems there is much less that can be justified rigorously. Nevertheless, estimators can still be constructed and if they perform well in calculations then they are useful for practical computations, see e.g. Mücke and Whiteman in [9] for an extension of an estimator used for linear elasticity to the finite elastic case. The estimator given in [9] is close to what we give here but the context and the route to obtaining the estimator are different. In [9] the estimator is for a compressible elastic material, the loading does not depend on the deformation and the derivation is based on expanding the total potential energy about the exact solution which gives the minimum. Here we have instead an incompressible membrane, pressure loading and to obtain the estimator we use a duality argument to relate a norm of the error $\underline{e} = \underline{u} - \underline{u}_h$ to an appropriate symmetric bilinear form of the type $\tilde{I}(\underline{e}, \underline{v})$ for appropriate functions $\underline{v}$. The details are as follows.

We first outline the procedure and then consider details specific to the membrane problem. With the exact solution $\underline{u} \in V$ satisfying (10) and the approximate solution $\underline{u}_h \in V_h \subset V$ satisfying (76) and with $\underline{e} := \underline{u} - \underline{u}_h$ we define

$$a_1(\underline{e}, \underline{v}) := a(\underline{u}_h + \underline{e}, \underline{v}) - a(\underline{u}_h, \underline{v}) = a(\underline{u}, \underline{v}) - a(\underline{u}_h, \underline{v}), \tag{79}$$
$$b_1(\underline{e}, \underline{v}) := b(\underline{u}_h + \underline{e}, \underline{v}) - b(\underline{u}_h, \underline{v}) = b(\underline{u}, \underline{v}) - b(\underline{u}_h, \underline{v}), \tag{80}$$
$$I(\underline{e}, \underline{v}) := a_1(\underline{e}, \underline{v}) - Pb_1(\underline{e}, \underline{v}) = -a(\underline{u}_h, \underline{v}) + Pb(\underline{u}_h, v) \tag{81}$$

and note that we have the Galerkin orthogonality type result

$$I(\underline{e}, \underline{v}) = 0 \quad \forall \underline{v} \in V_h. \tag{82}$$

The term $I(.,.)$ is nonlinear in the first argument and to proceed further we linearise about the approximate solution $\underline{u}_h$ by constructing symmetric bilinear forms $\tilde{a}_1(.,.)$, $\tilde{b}_1(.,.)$ and $\tilde{I}_1(.,.)$ such that for vectors $\underline{v}$ such that $\|\underline{v}\|$ is $\mathcal{O}(1)$ we have

$$a_1(\underline{e}, \underline{v}) = \tilde{a}_1(\underline{e}, \underline{v}) + \mathcal{O}(\|\underline{e}\|^2), \tag{83}$$
$$b_1(\underline{e}, \underline{v}) = \tilde{b}_1(\underline{e}, \underline{v}) + \mathcal{O}(\|\underline{e}\|^2) \tag{84}$$

and we define the bilinear form

$$\tilde{I}(\underline{e}, \underline{v}) := \tilde{a}_1(\underline{e}, \underline{v}) - P\tilde{b}_1(\underline{e}, \underline{v}) = -a(\underline{u}_h, \underline{v}) + Pb(\underline{u}_h, v) + \mathcal{O}(\|\underline{e}\|^2). \tag{85}$$

For the bilinear form $\tilde{I}(.,.)$ we have the approximate Galerkin orthogonality

condition

$$\tilde{I}(\underline{e},\underline{v}) = \mathcal{O}(\|\underline{e}\|^2) \quad \forall \underline{v} \in V_h \tag{86}$$

and if $\tilde{I}(.,.)$ is coercive on V then we can define a norm by

$$\|\underline{v}\|_M = (\tilde{I}(\underline{v},\underline{v}))^{1/2} \tag{87}$$

and we have

$$\|\underline{e}\|_M = \sup\{\tilde{I}(\underline{e},\underline{v}) : \ \underline{v} \in V, \ \|\underline{v}\|_M = 1\}. \tag{88}$$

Up to terms of $\mathcal{O}(\|\underline{e}\|^2)$ we can use standard arguments used for a linear problem to construct a bound for $\tilde{I}(\underline{e},\underline{v})$ for all vectors satisfying $\|\underline{v}\|_M = 1$ of the form

$$\|\underline{e}\|_M^2 \leq (\text{const}) \sum_{k=1}^{\text{ne}} \eta_k^2 \tag{89}$$

where η_k is the estimator on the kth triangle Ω_k involving residual quantities.

To describe $\tilde{a}_1(.,.)$ and $\tilde{b}_1(.,.)$ and to describe the estimator it is convenient to introduce the following vectors in $\mathbb{R}^6$

$$\hat{\underline{F}} = (F_{11}, F_{22}, F_{21}, F_{12}, F_{31}, F_{23})^T, \tag{90}$$

$$\hat{\nabla}\underline{v} = \left(\frac{\partial v_1}{\partial x_1}, \frac{\partial v_2}{\partial x_2}, \frac{\partial v_2}{\partial x_1}, \frac{\partial v_1}{\partial x_2}, \frac{\partial v_3}{\partial x_1}, \frac{\partial v_3}{\partial x_2}\right)^T, \tag{91}$$

$$\hat{\underline{\Pi}} = (\Pi_{11}, \Pi_{22}, \Pi_{21}, \Pi_{12}, \Pi_{31}, \Pi_{23})^T, \tag{92}$$

corresponding to the tensors $\mathbf{F}$, $\nabla\underline{v}$ and $\mathbf{\Pi}$ in $\mathbb{R}^{3,2}$. We also introduce the norm notation

$$\|\underline{v}\|_G^2 = \iint_G |\underline{v}|^2 \, dx_1 dx_2 \quad \text{and} \quad \|\underline{v}\|_{\partial G}^2 = \int_{\partial G} |\underline{v}|^2 \, \mathrm{d}s \tag{93}$$

for any region $G \subset \mathbb{R}^2$.

For $\tilde{a}_1(\underline{e},\underline{v})$ we have for our hyperelastic material with strain energy function W in this membrane case that

$$a_1(\underline{e},\underline{v}) = a(\underline{u}_h + \underline{e},\underline{v}) - a(\underline{u}_h,\underline{v}) = a(\underline{u},\underline{v}) - a(\underline{u}_h,\underline{v}) \tag{94}$$

$$= \iint_\Omega \left(\frac{\partial W}{\partial \hat{\underline{F}}}(\hat{\underline{F}}(\underline{u})) - \frac{\partial W}{\partial \hat{\underline{F}}}(\hat{\underline{F}}(\underline{u}_h)\right) \cdot \hat{\nabla}\underline{v} \, dx_1 dx_2 \tag{95}$$

$$\approx \iint_\Omega \hat{\nabla}\underline{e}^T D(\hat{\underline{F}}(\underline{u}_h)) \hat{\nabla}\underline{v} \, dx_1 dx_2 =: \tilde{a}_1(\underline{e},\underline{v}) \tag{96}$$

where D is the 6×6 Hessian matrix with entries

$$D_{ij} = \frac{\partial^2 W}{\partial(\hat{\underline{F}})_i \partial(\hat{\underline{F}})_j}. \tag{97}$$

$\tilde{a}_1(.,)$ is clearly a symmetric bilinear form.

To describe $\tilde{b}_1(.,.)$ we refer directly to the definition of $b(.,.)$ to get

$$b_1(\underline{e},\underline{v}) = b(\underline{u},\underline{v}) - b(\underline{u}_h,\underline{v}) \tag{98}$$

$$\approx \iint_\Omega \underline{v}\cdot\left(\frac{\partial \underline{w}_h}{\partial x_1}\times\frac{\partial \underline{e}}{\partial x_2}\right)+\left(\frac{\partial \underline{e}}{\partial x_1}\times\frac{\partial \underline{w}_h}{\partial x_2}\right)\,dx_1dx_2 =: \tilde{b}_1(\underline{e},\underline{v}). \tag{99}$$

To obtain the bound (89) we need a coercive property of the form

$$\|\underline{v}\|_M^2 = \tilde{I}(\underline{v},\underline{v}) \geq \sum_{k=1}^{\mathrm{ne}} \alpha_k^2 \|\hat{\nabla}\underline{v}\|_{\Omega_k}^2. \tag{100}$$

Whether or not this is true depends on the form of W and on the displacement field $\underline{u}_h$ that is obtained and the possibility that this is not true in many cases is one of the main difficulties in doing rigorous analysis for these nonlinear problems.

Finally, to obtain the expression for the estimator η_k we need to consider the term $\tilde{I}(\underline{e},\underline{v})$. First observe that $\tilde{I}(\underline{e},\underline{v}) = I(\underline{e},\underline{v}) + \mathcal{O}(\|\underline{e}\|^2)$ and from (81), that $\mathbf{\Pi}_h = \mathbf{\Pi}(\underline{u}_h)$ is constant interior to a triangle and the divergence theorem we obtain the representation

$$I(\underline{e},\underline{v}) = \sum_{k=1}^{\mathrm{ne}}\left\{\iint_\Omega -P\underline{v}\cdot\left(\frac{\partial \underline{w}_h}{\partial x_1}\times\frac{\partial \underline{w}_h}{\partial x_2}\right)\,dx_1dx_2 + \int_{\partial\Omega_k}\underline{v}\cdot(\mathbf{\Pi}_h^T\underline{N})\,\mathrm{d}s\right\} \tag{101}$$

$$= \sum_k\left\{\iint_{\Omega_k}\underline{v}\cdot\underline{S}_h\,dx_1dx_2 + \frac{1}{2}\int_{\partial\Omega_k}\underline{v}\cdot\underline{J}_h\,\mathrm{d}s\right\} \tag{102}$$

$$= \sum_k\left\{\iint_{\Omega_k}(\underline{v}-\underline{v}_h)\cdot\underline{S}_h\,dx_1dx_2 + \frac{1}{2}\int_{\partial\Omega_k}(\underline{v}-\underline{v}_h)\cdot\underline{J}_h\,\mathrm{d}s\right\}, \tag{103}$$

for all $\underline{v}_h \in V_h$, where

$$\underline{S}_h := P\left(\frac{\partial \underline{w}_h}{\partial x_1}\times\frac{\partial \underline{w}_h}{\partial x_2}\right), \tag{104}$$

$$\underline{J}_h := \left(\mathbf{\Pi}^T(\underline{u}_h)|_{\Omega_k} - \mathbf{\Pi}^T(\underline{u}_h)|_{\Omega_{k'}}\right)\underline{N}, \tag{105}$$

where in (105) Ω_k and $\Omega_{k'}$ share an edge and where (103) follows from (102) using the orthogonality relation (82).

Using shape regular meshes throughout there exists, as stated in Braess [2, p.172] a constant C, depending only on the mesh, and a function $\underline{v}_h \in V_h$ such that for all triangles Ω_k in the mesh we have

$$\|\underline{v}-\underline{v}_h\|_{\Omega_k} \leq Ch_k\|\hat{\nabla}\underline{v}\|_{\omega(\Omega_k)}, \quad \|\underline{v}-\underline{v}_h\|_{\partial\Omega_k} \leq Ch_k^{1/2}\|\hat{\nabla}\underline{v}\|_{\omega(\Omega_k)}, \tag{106}$$

where h_k is the size of the triangle Ω_k and where $\omega(\Omega_k)$ is the union of all triangles which have at least one node in common with Ω_k. Then by using the Cauchy-Schwarz inequality on the area integral and on the boundary integral we have

$$I(\underline{e},\underline{v}) \leq C \sum_k \|\hat{\nabla}\underline{v}\|_{\omega(\Omega_k)} \left(\|h_k \underline{S}_h\|_{\Omega_k} + \frac{1}{2}\|h_k^{1/2}\underline{J}_h\|_{\partial\Omega_k} \right) \tag{107}$$

$$= C \sum_k \alpha_k \|\hat{\nabla}\underline{v}\|_{\omega(\Omega_k)} \left(\frac{\|h_k \underline{S}_h\|_{\Omega_k}}{\alpha_k} + \frac{1}{2}\frac{\|h_k^{1/2}\underline{J}_h\|_{\partial\Omega_k}}{\alpha_k} \right) \tag{108}$$

assuming the validity of the coercive property. Then by using the Cauchy-Schwarz inequality for sums on the smooth part and the jump part separately we have

$$\tilde{I}(\underline{e},\underline{v}) \leq C \left(\sum_k \alpha_k^2 \|\hat{\nabla}\underline{v}\|^2_{\omega(\Omega_k)} \right)^{1/2} \left\{ \left(\sum_k \frac{\|h_k \underline{S}_h\|^2_{\Omega_k}}{\alpha_k^2} \right)^{1/2} + \frac{1}{2} \sum_k \left(\frac{\|h_k^{1/2}\underline{J}_h\|^2_{\partial\Omega_k}}{\alpha_k^2} \right)^{1/2} \right\} \tag{109}$$

Now for any positive numbers β and γ we have

$$(\beta+\gamma/2)^2 = \beta^2+\gamma^2/4+\beta\gamma \leq \beta^2+\gamma^2/4+\frac{1}{2}(\beta^2+\gamma^2) = \frac{3}{2}(\beta^2+\gamma^2/2). \tag{110}$$

Applying this to the part $\{.\}$ in (109) and absorbing the factor $(3/2)^{1/2}$ in the constant C gives

$$I(\underline{e},\underline{v}) \leq C \left(\sum_k \alpha_k^2 \|\hat{\nabla}\underline{v}\|^2_{\omega(\Omega_k)} \right)^{1/2} \left(\sum_k \left\{ \frac{h_k^2 \|\underline{S}_h\|^2_{\Omega_k}}{\alpha_k^2} + \frac{1}{2}\frac{h_k \|\underline{J}_h\|^2_{\partial\Omega_k}}{\alpha_k^2} \right\} \right)^{1/2}. \tag{111}$$

Now when we have the coercive property (100) and we restrict to vectors $\underline{v}$ satisfying $\|\underline{v}\|_M = 1$ it follows that there exists a constant $C_M \geq 1$ such that

$$\sum_k \alpha_k^2 \|\hat{\nabla}\underline{v}\|^2_{\omega(\Omega_k)} \leq C_M. \tag{112}$$

Using this result, (111) and (88) gives

$$\|\underline{e}\|_M \leq C C_M \left(\sum_{k=1}^{\text{ne}} \tilde{\eta}_k^2 \right)^{1/2} \quad \text{where} \quad \alpha_k^2 \tilde{\eta}_k^2 = h_k^2 \|\underline{S}_h\|^2_{\Omega_k} + \frac{1}{2} h_k \|\underline{J}_h\|^2_{\partial\Omega_k}. \tag{113}$$

The term $\tilde{\eta}_k$ just defined is a possible estimator that we can use on the kth triangle. However, as given, it requires the computation of α_k^2 which can be

estimated by computing the eigenvalues of D. From the definition of $\tilde{a}_1(.,.)$ we have the Rayleigh quotient bound

$$\tilde{a}_1(\underline{v},\underline{v}) = \sum_k \iint_{\Omega_k} (\hat{\nabla}\underline{v})^T D_k \hat{\nabla}\underline{v}\, dx_1 dx_2 \geq \sum_k \lambda_{\min}(D_k) \|\hat{\nabla}\underline{v}\|^2_{\Omega_k} \tag{114}$$

and by using the definition of $\tilde{b}_1(\underline{v},\underline{v})$ it follows that we can take

$$\alpha_k^2 = \lambda_{\min}(D_k) - P|\underline{w}_h|_k, \tag{115}$$

where here $|\underline{w}_h|_k$ is the furthest point on Ω_k from the origin, provided the right hand side is positive for the given deformation. For practical computations we can of course always just compute instead the quantities

$$\eta_k^2 = h_k^2 \|\underline{S}_h\|^2_{\Omega_k} + \frac{1}{2} h_k \|\underline{J}_h\|^2_{\partial\Omega_k}, \quad k = 1, 2, \cdots, \text{ne} \tag{116}$$

as a guide to the distribution of the error over the domain. This simplistic approach is what is done in our computations.

5 Numerical results

In this section we consider a few points concerning the detail of the implementation of our model and we show some typical results that we obtain. Some finer points of the detail are important to a 'satisfactory simulation' and these concern how we make use of the residual estimator described in section 4 and with how we automatically determine the time step to use.

As we have a membrane model the deformation just depends on the ratio of the applied pressure P to the initial thickness h_0 and thus, without loss of generality we can set $h_0 = 1$. We assume that the pressure increases with time t according to $P(t) = t$. We assume throughout that both elastic springs in figure 1 satisfy the same Jones-Treloer relations corresponding to

$$\begin{aligned} W_1 = &\frac{0.69}{1.3}(\lambda_1^{1.3} + \lambda_2^{1.3} + \lambda_1^{-1.3}\lambda_2^{-1.3} - 3) + \frac{0.01}{4}(\lambda_1^4 + \lambda_2^4 + \lambda_1^{-4}\lambda_2^{-4} - 3) \\ &+ \frac{0.0122}{2}(\lambda_1^2 + \lambda_2^2 + \lambda_1^{-2}\lambda_2^{-2} - 3) \end{aligned} \tag{117}$$

where λ_1^2 and λ_2^2 are the eigenvalues of $\mathbf{C}$. In the case of W_2 we have the same form with λ_1 and λ_2 replaced by $\tilde{\lambda}_1$ and $\tilde{\lambda}_2$ respectively where $\tilde{\lambda}_1^2$ and $\tilde{\lambda}_2^2$ are the eigenvalues of $\mathbf{C}\,\mathbf{A}^{-1}$. (This is different to what is given in [6,7] where the spring in branch 2 is of the neo-Hookean form.) With these parameters a large part of the deformation occurs in the time $0 \leq t \leq 3$ with a much

higher pressure required to force all the nodes against the mould for the geometries considered here. For the viscosity parameter ν we take $\nu = 0.1$ in these calculations. In each case we start with a uniform mesh of the domain Ω, we assume a uniform prestretch of magnitude 1.2 in the x and y directions, we assume that the sheet is then clamped around the edge and the pressure is applied until all the nodes come into contact with the mould by solving at a sequence of time levels $0 = t_0 < t_1 < t_2 < \cdots$. These time levels are increased or decreased so that we have the following.

(i) As stated in section 3 we half the time step if the Newton iteration at time t_i does not converge.

(ii) If for a given value of $\delta > 0$ the iteration converges at time t_i and we obtain a solution for which

$$\max\{|\underline{u}(\underline{x}_k, t_i) - \underline{u}(\underline{x}_k, t_{i-1})| : \ \underline{x}_k \text{ is a node}\} > \delta \tag{118}$$

then we reject the solution and half the time step to better determine what happens between times t_{i-1} and t_i. This increases the accuracy in the predictor–corrector scheme and it is also important for determining where points come into contact with the mould. If δ is too large here then we may inaccurately predict where points come into contact with the mould at some stages. We have used $\delta = 0.025$ in the results presented here. With this choice the situation described in (i) did not occur.

(iii) Conversely to (ii) we increase the time step for the next time level if the maximum change over all the nodes from time t_{i-1} to time t_i is very small. This is important in practical computations to quickly reach the stage when all nodes are in contact with the mould.

The error estimators $\eta_1^2, \eta_2^2, \cdots, \eta_{\rm ne}^2$ defined in (116) are computed at each time level t_i although we only refine the mesh once when all the deformed nodes are in contact with the mould if we are going to repeat the computation. This is the simplest and the most satisfactory of the strategies that we have tried. Other strategies such as possibly refining from one time level to the next, which may involve many refinements in total, are more complicated as they require that data is transferred between meshes. With the strategy that we are using involving re-computing the complete process with a finer mesh it should be noted that the early runs with relatively coarse meshes only take a small proportion of the total time taken.

When a complete run is done the decision as to which triangles to refine ready for a repeat of the computation can be a delicate matter with each different strategy leading to different meshes and slightly different results. At any given stage the quantities η_k^2 are only for the values of k corresponding to triangles which are not yet stuck to the mould and which values are computed changes as the process proceeds. Also, for the kth triangle the quantity η_k^2 generally increases with the time level as in particular $\underline{S}_h$ defined in (104) contains the

factor $P(t_i)$ and the other term given in (105) is also likely to increase with $P(t_i)$. To take these factors into account to decide which triangles to refine we compute

$$E_k = \frac{\eta_k^2}{P(t_i)^2}, \quad k = 1, 2, \cdots, \text{ne} \tag{119}$$

once a solution is obtained at time t_i. For a given value of $\epsilon > 0$ we refine element k at the end of the run if $E_k > \epsilon$ at any of the time levels $t_1 < t_2 < \cdots$. In the results presented in the figures that follow we have fairly arbitrarily taken $\epsilon = 10^{-3}$ and we have repeated the run up to 4 times. This rather simplistic and crude approach seems to work remarkably well in picking out the parts of the sheet which makes contact with the more difficult geometrical parts of the mould.

In figure 2 the mould is the box shape with interior

$$\{-1.2 < x, y < 1.2, \quad 0 < z < 1.2\} \tag{120}$$

and we show the mesh after 4 levels of refinement and the final deformed shape obtained. The results are as you might expect with the finest part of the mesh corresponding to where sheet makes contact with the corners of the mould. As the domain has symmetry the computation is done with a symmetric 1/8th of the domain. The first mesh is a uniform mesh of 256 triangles and the next 3 meshes have 883, 1109 and 1115 triangles. For the presentation the mesh shown in figure 2 has $8 \times 1115 = 8920$ triangles.

In figure 3 we show a similar mould shape corresponding to the interior

$$\{-2.4 < x < 2.4, \quad -1.2 < y < 1.2, \quad 0 < z < 1.2\} \tag{121}$$

which has fold symmetry. The results are similar to the box shape and we include it here in order to comment upon the refinement which is done in the centre of the region. This is not really needed and is as a consequence of the criterion we have described, the mould shape and the contact algorithm. With this geometry the sheet first makes contact with the mould at the centre with many nodes coming into contact at the same time. The process of moving the nodes back to the mould and with then re-establishing equilibrium can sometimes lead to above average values of η_k^2 for the triangles involved which are thus marked for refinement for the next run. This unfortunate feature can be removed by reducing the value of δ given in (118) but this leads to more time steps being needed and a greater computation time. The mesh shown has 3563 triangles in a symmetric quarter of the the domain. The 3 previous meshes in the sequence have 1024, 3248 and 3547 elements.

In figure 4 we show the results for the box-on-box shape which has the interior

$$\{-1.2 < x, y < 1.2,\ 0 < z < 1.2\} \cup \{-0.8 < x, y < 0.8,\ 1.2 \leq z < 1.8\}. \tag{122}$$

As with the box shape we can do the computations with a symmetric 1/8th of the domain and the sequence of meshes used involved 256, 917, 1606 and 1976 triangles. The refinement procedure does remarkably well here.

Finally in figure 5 we increase the mould complexity further by giving the results for a cylinder on a box on a box. The interior of this shape is the same as (122) with in addition the cylinder part at the top having the interior

$$\{0 \leq \sqrt{x^2 + y^2} < 0.4,\ 1.8 \leq z < 2.4\}. \tag{123}$$

Again, because of the symmetry, we only need to consider a symmetric 1/8th of the domain. The sequence of meshes used had 256, 917, 1600 and 2195 triangles. As in the previous example the refinement procedure does remarkably well here.

As final comments here, the algorithm involving solving the nonlinear system arising from the finite element spatial discretization combined with the predictor corrector scheme to determine how $\mathbf{A}(t)$ evolves in time works smoothly throughout. When the full Newton method is used to solve the nonlinear equations we typically only need about half the number of iterations to perform the corrector step as compared with the predictor step at each time level. All the computations that we have done suggests that the time discretization error is small compared with the spatial errors which is probably mainly as a consequence of choosing $\delta > 0$ small enough so restricting the amount of change between time levels. Also, we must report that the computation done using a range of values of the viscosity parameter ν all lead to final displacement fields which are close as is also reported in [7] which suggests that the viscoelastic properties of the materials are not among the more important features to consider when modelling thermoforming when only displacements are required. This outcome in this modelling set-up is not understood.

6 Conclusions

This paper extends a finite viscoelastic model introduced by Le Tallec in [6], and used previously in the thermoforming context in [7], to allow for any type of elastic springs in a spring and dashpot set-up. This paper also derives, and partly justifies, a residual based error estimator for use in finite elastic and finite viscoelastic problems involving incompressible membranes. Although we are not able to guarantee the accuracy of any of the results presented, the numerical results are quite impressive in terms of the meshes generated corresponding to the more difficult geometrical features. On the computational side future improvements here need to concentrate on improving the efficiency of the algorithm further and with being able to better guarantee the accuracy

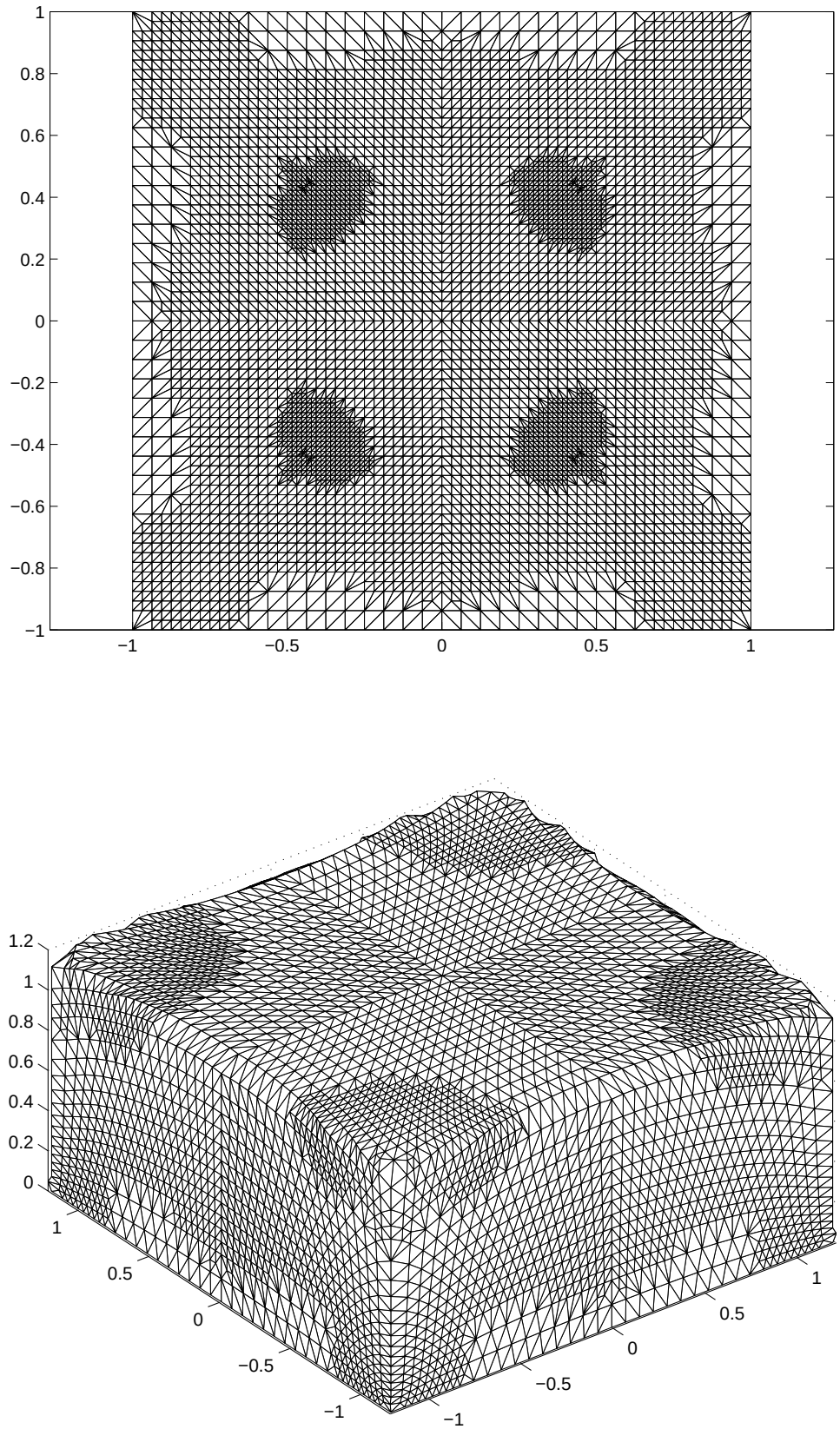

Fig. 2. Box shape: The mesh shown has $8 \times 1115 = 8920$ triangles

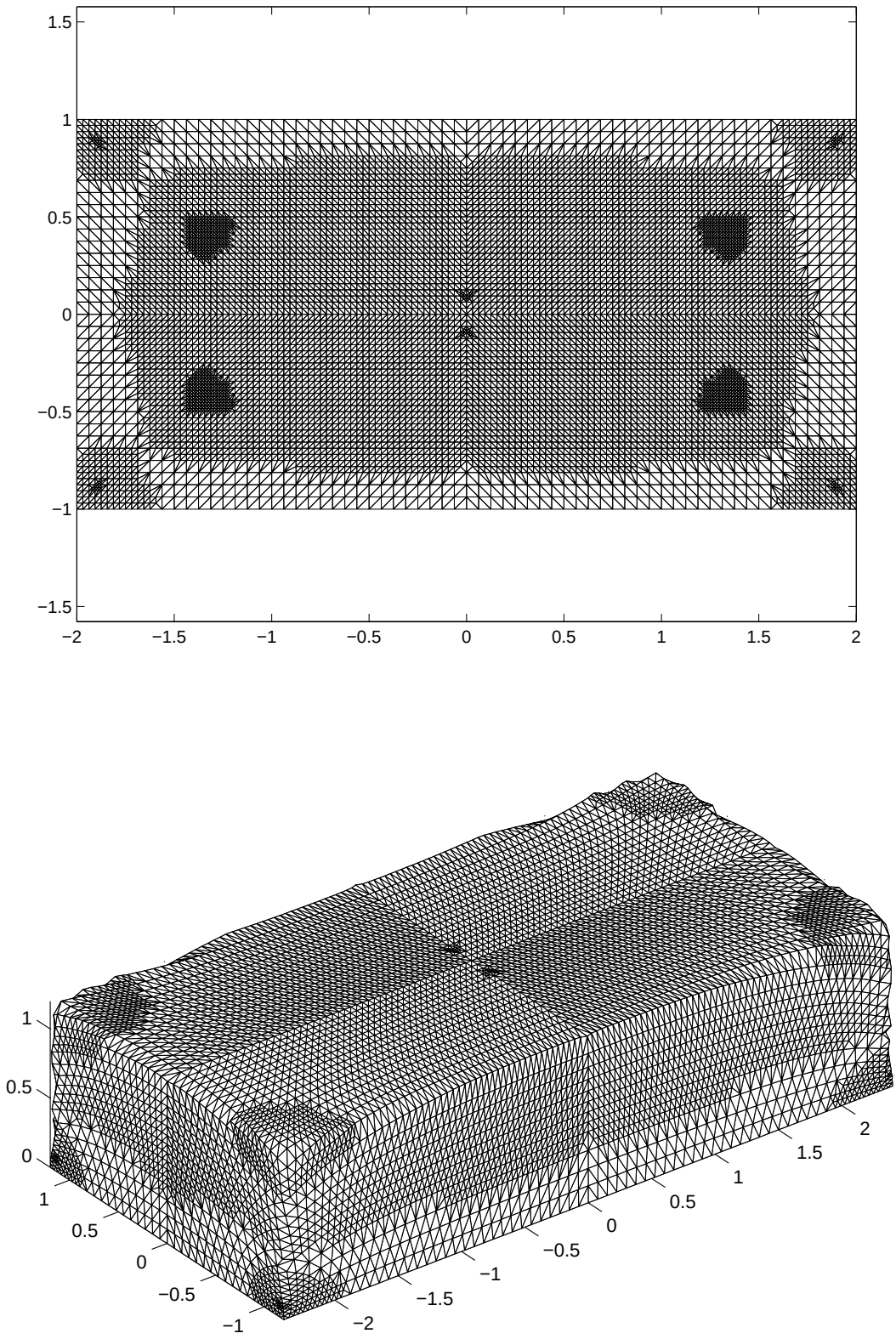

Fig. 3. Rectangular shape: The mesh shown has $4 \times 3563 = 14252$ triangles.

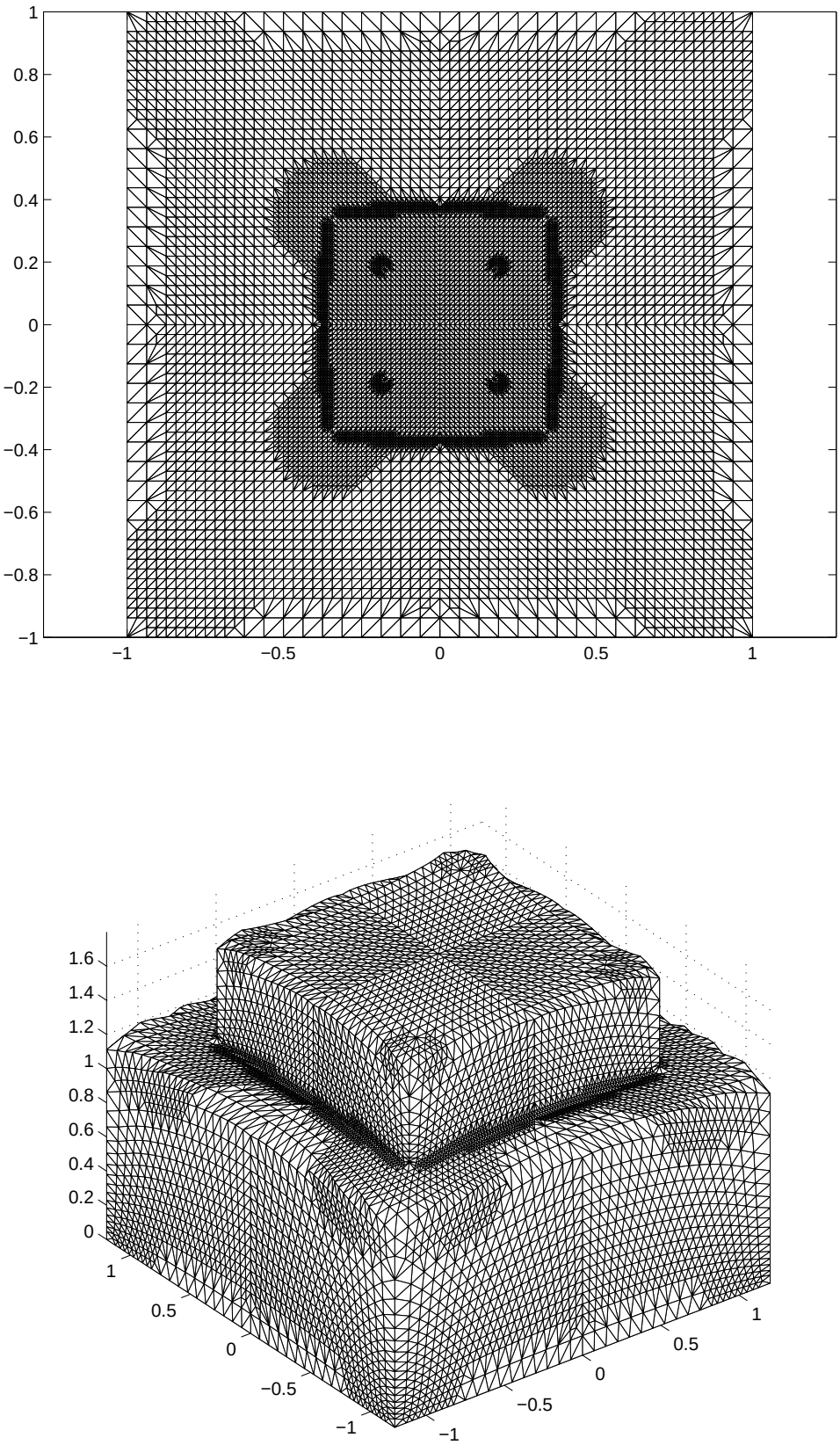

Fig. 4. Box-on-box shape: The mesh shown has 8×1976 triangles.

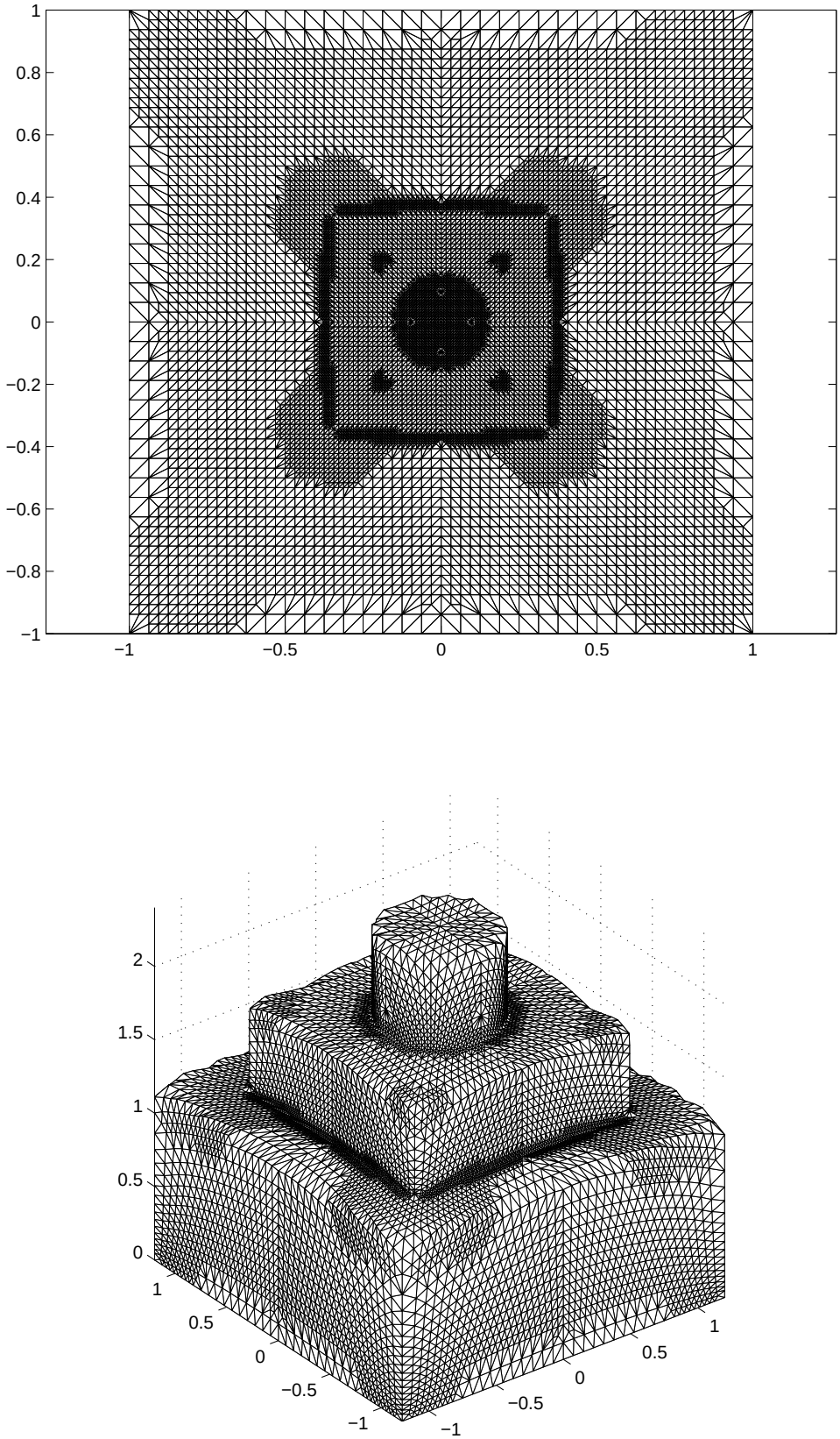

Fig. 5. Cylinder-on-box-on-box shape: The mesh shown has 8×2195 triangles.

of what is computed.

References

[1] H. Andrä, M. Warby, and J.R. Whiteman. Contact problems of hyperelastic membranes: existence theory. *Mathematical methods in the applied sciences*, 23(10):865–895, July 2000.

[2] D. Braess. *Finite Elements, theory, fast solvers, and applications in solid mechanics*. Cambridge, second edition, 2001.

[3] R.M. Christensen. A non-linear theory of viscoelasticity for application to elastomers. *Journal of applied mechanics*, 47:762–768, 1980.

[4] H. DeLorenzi and C.A. Nied, H.and Taylor. Simulation and analysis of blow molding using the finite element method. *ANTEC*, pages 797–799, 1988.

[5] W.G. Jiang, M.K. Warby, J.R. Whiteman, S. Abbott, W. Shorter, P. Warwick, T. Wright, A. Munro, and B. Munro. Finite element modelling of high air pressure forming processes for polymer sheets. *Computational Mechanics*, 31:163–172, 2003.

[6] P. Le Tallec and C. Rahier. Numerical models of steady rolling for non-linear viscoelastic structures in finite deformations. *International journal for numerical methods in engineering*, 37:1159–1186, 1994.

[7] Karamanou M., Shaw S., Warby M.K., and Whiteman J.R. Model, algorithms and error estimation for computational viscoelasticity. *Comput. Methods Appl. Mech. Engrg.*, 194:245–265, 2005.

[8] L. E. Malvern. *Introduction to the mechanics of a continuous medium*. Prentice-Hall, 1969.

[9] R. Mücke and J.R. Whiteman. A posteriori error estimates and adaptivity for finite element solutions in finite elasticity. *International journal for numerical methods in engineering*, 38:775–795, 1995.

[10] C.A. Nied, H.and Taylor and H. DeLorenzi. Three-dimensional finite element simulation of thermoforming. *Polymer Engineering and Science*, 30(20):1314–1322, 1990.

[11] C.A. Taylor, H. DeLorenzi, and D.O. Kazmer. Experimental and numerical investigations of the vacuum-forming process. *Polymer Engineering and Science*, 32(16):1163–1173, 1992.

[12] C.A. Taylor, H. DeLorenzi, and H. Nied. Finite element simulation of thermoforming-experiments and analyses. *ANTEC*, pages 435–437, 1989.

[13] M.K. Warby, J.R. Whiteman, W.G. Jiang, P. Warwick, and T. Wright. Finite element simulation of thermoforning processes for polymer sheets. *Mathematics and Computers in Simulation*, (61):209–218, 2003.